

RESEARCH ARTICLE

10.1029/2018JD029142

Key Points:

- No summer cloud-sea ice feedback emerges in a global climate model in a future sea ice-free Arctic
- Future fall clouds become more opaque and the boundary layer deepens over newly open water
- Annual net Arctic cloud-sea ice feedback is positive but the magnitude may be underestimated in this study

Correspondence to:

A. L. Morrison,
ariel.morrison@colorado.edu

Citation:

Morrison, A. L., Kay, J. E., Frey, W. R., Chepfer, H., & Guzman, R. (2019). Cloud response to Arctic Sea ice loss and implications for future feedback in the CESM1 climate model. *Journal of Geophysical Research: Atmospheres*, 124. <https://doi.org/10.1029/2018JD029142>

Received 7 JUN 2018

Accepted 1 DEC 2018

Accepted article online 10 DEC 2018

Cloud Response to Arctic Sea Ice Loss and Implications for Future Feedback in the CESM1 Climate Model

A. L. Morrison^{1,2} , J. E. Kay^{1,2} , W. R. Frey^{1,2} , H. Chepfer^{3,4} , and R. Guzman³ 

¹Atmospheric and Oceanic Sciences, University of Colorado Boulder, Boulder, Colorado, USA, ²Cooperative Institute for Research in Environmental Sciences, University of Colorado Boulder, Boulder, Colorado, USA, ³LMD/IPSL, CNRS, Ecole Polytechnique, Palaiseau, France, ⁴LMD/IPSL, Université Pierre et Marie Curie, Paris, France

Abstract Over the next century, the Arctic is projected to become seasonally sea ice-free. Assessing feedback between clouds and sea ice as the Arctic loses sea ice cover is important because of clouds' radiative impacts on the Arctic surface. Here we investigate present-day and future Arctic cloud-sea ice relationships in a fully coupled global climate model forced by business-as-usual increases in greenhouse gases. Model evaluation using a lidar simulator and lidar satellite observations shows agreement between present-day modeled and observed cloud-sea ice relationships. Summer clouds are unaffected by sea ice variability, but more fall clouds occur over open water than over sea ice. Because the model reproduces observed cloud-sea ice relationships and their underlying physical mechanisms, the model is used to assess future Arctic cloud-sea ice feedback. With future sea ice loss, modeled summer cloud fraction, vertical structure, and optical depth barely change. Future sea ice loss does not influence summer clouds, but summer sea ice loss does drive fall cloud changes by increasing the amount of sunlight absorbed by the summertime ocean and the latent and sensible heat released into the atmosphere when the Sun sets in fall. The future fall boundary layer deepens and clouds become more opaque over newly open water. The future nonsummer longwave cloud radiative effect strengthens as nonsummer cloud cover increases. In summary, we find no evidence for a summer cloud-sea ice feedback but strong evidence for a positive cloud-sea ice feedback that emerges during nonsummer months as the Arctic warms and sea ice disappears.

1. Introduction

The Arctic is warming and losing sea ice cover in response to increasing anthropogenic greenhouse gas emissions (Bindoff et al., 2013). Arctic warming and sea ice loss are projected to continue, in part because of positive feedback associated with sea ice loss (Serreze & Barry, 2011). Sea ice loss can affect other components of the Arctic climate system by modifying heat and moisture fluxes from the ocean to the atmosphere (e.g., Boisvert & Stroeve, 2015; Lawrence et al., 2008; Morrison et al., 2018). As the Arctic Ocean transitions toward an increasingly ice-free state, understanding Arctic climate feedback and their changes in response to sea ice loss is necessary for predicting future climate.

It is particularly important to isolate how cloud-sea ice feedback may change in a warming Arctic. Through their radiative influence on the surface, Arctic clouds can enhance or mitigate Arctic warming (Shupe & Intrieri, 2004) and impact the rate of Arctic sea ice loss (e.g., Choi et al., 2014; Kay, Holland, et al., 2012; Winton, 2006). Clouds containing liquid water, instead of just ice crystals, dominate clouds' radiative impact on the Arctic surface (Shupe & Intrieri, 2004). When the cloud response to sea ice loss is isolated from other cloud-controlling factors, there is no observed change in cloud fraction, structure, or opacity when sea ice cover is lost during summer (June–July–August; see Kay, L'Ecuyer, et al., 2016 review paper). In other words, one bright reflective surface (sea ice) is not being replaced by another (clouds) during the summer. Since there is no observed summer cloud response to sea ice loss, there is no observational evidence for a shortwave summer cloud-sea ice feedback in the current Arctic climate. In contrast, observations do show more clouds over newly open water during the fall (September–October–November; see Kay, L'Ecuyer, et al., 2016 review paper). In other words, a cloud feedback due to sea ice loss does occur during the fall. As the Arctic rapidly transitions to a seasonally ice-free state, assessing if observed present-day cloud-sea ice relationships inform future cloud-sea ice feedback is an important and unanswered question.

While observations can constrain present-day cloud-sea ice relationships, theory and models are required to project future cloud-sea ice relationships as the Arctic Ocean transitions to increasingly open water

conditions. Representing clouds in numerical models is challenging, but models built using physical understanding can be used to investigate the influence of global warming on cloud properties and feedback (Boucher et al., 2013). Most models agree that globally the longwave (Soden & Vecchi, 2011) and high cloud feedback will be positive (Zelinka et al., 2012). In contrast, the magnitude and sometimes even the sign of the shortwave (Ceppi et al., 2016; Soden & Vecchi, 2011) and low cloud feedback remain poorly constrained (Gordon & Klein, 2014). Unfortunately, the current generation of climate models does not agree on the sign of the net cloud feedback in the Arctic, highlighting the difficulty of analyzing Arctic cloud feedback in models. For example, Zelinka et al. (2012) found that a negative cloud feedback emerges over the Arctic Ocean as cloud optical depth increases with warming in the multimodel mean of Coupled Model Intercomparison Projection version 5 (CMIP5) models, but Pithan and Mauritsen (2014) found that the CMIP5 multimodel mean Arctic cloud feedback is positive as increasing cloud thickness and amount warm the surface for most of the year. In both studies there was intermodel disagreement on the sign of the Arctic cloud-climate feedback.

Modeling has helped improve physical understanding of the mechanisms underlying Arctic cloud feedback and their relationship to sea ice loss. In the Arctic, previous modeling studies have reported low cloud increases as sea ice is lost in nonsummer months. These nonsummer cloud increases were attributed to increased moisture fluxes from the ocean as sea ice concentration decreases (e.g., Kay et al., 2011; Vavrus et al., 2009; Vavrus et al., 2011) and lead to a positive cloud feedback. During summer, previous modeling studies have also found increases in summertime Arctic Ocean cloud cover over the twenty-first century (e.g., Koenig et al., 2013; Vavrus et al., 2009) and at times highly unrealistic modeled summer cloud responses to summer sea ice loss (e.g., Kay et al., 2011).

Building on existing research and motivated by the need to further constrain the sign of Arctic cloud-sea ice feedback, this study has three goals: (1) evaluate present-day Arctic cloud sea ice relationships in a global climate model using state-of-the-art observations and comparison techniques, (2) evaluate if the mechanisms controlling present-day cloud-sea ice relationships and the lack of an observed summer cloud-sea ice feedback are still relevant in a future sea ice free Arctic, and (3) assess the sign and strength of future Arctic cloud-sea ice feedback. These three goals are highly related. We understand present-day observed cloud-sea ice relationships and we have the tools needed to evaluate these relationships in models (e.g., the intermittent mask described in Morrison et al., 2018; satellite simulators described in Bodas-Salcedo et al., 2011). Models are most useful when they reproduce observations for the right physical reasons. Thus, we must ensure that the model reproduces observed relationships between present-day clouds and sea ice for the right physical reasons before using the model to understand future sea ice-cloud relationships and to assess the sign of future sea ice-cloud feedback.

2. Methods

2.1. CESM1 Simulations

In this study, we use a fully coupled ocean-atmosphere-land-sea ice-biogeochemistry Earth system model: Community Earth System Model version 1 with the Community Atmosphere Model version 5 (CESM1-CAM5) at a roughly 1° resolution (Hurrell et al., 2013). The ocean component of CESM1 is the Parallel Ocean Program version 2 (POP2), which has 60 vertical levels of varying depths (Smith et al., 2010). The sea ice component is the Community Ice Code version 4 (CICE4; Bailey et al., 2011). The atmospheric component of CESM1-CAM5 is the Community Atmospheric Model version 5 (CAM5), which includes atmospheric chemistry and extends into the lower thermosphere (~140 km above sea level; Neale et al., 2012). CESM1 is a widely used climate model and participated in CMIP5 (Taylor et al., 2012). CESM1 has been used extensively to study Arctic climate change (e.g., Barnhart et al., 2016; Blackport & Kushner, 2017; Jahn, 2018). Of relevance to this study, CESM1 can reproduce observed Arctic warming and sea ice loss (Jahn, 2018; Stroeve et al., 2012) but has insufficient Arctic cloud radiative forcing (Kay, Bourdages, et al., 2016).

Critical to this study, we use the Cloud Feedback Model Intercomparison Project Observational Simulator Package, COSP (Bodas-Salcedo et al., 2011). The instrument simulators contained within COSP enable scale-aware and definition-aware comparisons between modeled and observed clouds from many types of passive and active sensors. This study relies extensively on the lidar simulator contained within COSP (Chepfer et al., 2008). Modeled clouds are compared with an observational product designed specifically

for evaluation of climate models using COSP: CALIPSO-GOCCP (Cloud-Aerosol Lidar and Infrared Pathfinder Satellite GCM-Oriented CALIPSO Cloud Product, version 3.1.2; Chepfer et al., 2010). We use COSP1.4, which has cloud phase diagnostics (Cesana & Chepfer, 2013; Kay, Bourdages, et al., 2016). Since optically opaque clouds (optical depth > 3 (Chepfer et al., 2013)) dominate clouds' radiative effect on the surface (Curry & Ebert, 1992; Shupe & Intrieri, 2004) and top of the atmosphere (Vaillant de Guelis et al., 2017), we also use new cloud opacity diagnostics (Guzman et al., 2017) to evaluate changes in opaque clouds within the simulator framework.

The model simulation analyzed here is a single CESM1 simulation from 2006 to 2100 under Representative Concentration Pathway 8.5 forcing ("business-as-usual" emissions scenario). The simulation was initialized with restarts from member 1 from the CESM-Large Ensemble (CESM-LE) project (Kay et al., 2015). We use the CESM-LE code base but we updated COSP from the default of COSP1.3 (Kay, Hillman, et al., 2012) to COSP1.4 (Kay, Bourdages, et al., 2016) and also added new lidar opacity diagnostics (Guzman et al., 2017). Results are from daily mean outputs unless otherwise stated. Because we use daily output, we set the number of subcolumns in the subcolumn generator within COSP to 250. Unless otherwise stated, our analysis focuses on the present-day (2006–2015) and three 20-year future periods (2020–2039, 2050–2069, and 2080–2099).

2.2. Analysis Techniques for Assessing Cloud-Sea Ice Relationships in CESM1 Simulations

The analysis techniques we use to assess cloud-sea ice relationships are mostly standard, but our method for isolating the cloud response to sea ice variability requires further explanation. Following Morrison et al. (2018), we create two surface masks for summer and fall to restrict our analysis to regions of the Arctic Ocean where present-day daily mean sea ice concentrations vary. The first is the perennial mask, which is the region excluded from this study. The perennial mask includes all grid boxes where the daily mean sea ice concentration is < 15 or $> 80\%$ every day from 2006 to 2015. In other words, we exclude all grid boxes where sea ice concentration does not vary from 2006 to 2015. Sea ice concentration in a grid box must be < 15 or $> 80\%$ every day to be included in the perennial mask, so we do not average any daily sea ice concentrations to create the perennial mask. The intermittent mask is the analysis region for this study. The intermittent mask includes all grid boxes *not* in the perennial mask—specifically, grid boxes where the daily mean sea ice concentration is between 15 and 80% for at least one day from 2006 to 2015. Since sea ice exists within the intermittent mask in the present, sea ice can be lost within the intermittent mask in the future. Each season has its own intermittent mask because sea ice concentrations vary between seasons. The same seasonal intermittent masks, based on present-day daily sea ice concentrations, are used for all present-day and future CESM1 simulations to keep the present-day and future analysis regions constant. We create an annual intermittent mask as well. Overall, the intermittent masks in CESM1 are very similar to the intermittent masks from observations (Morrison et al., 2018). All results shown are based on output from within the CESM1 intermittent mask.

2.3. Analysis Techniques for Assessing Future Feedback in CESM1 Simulations

We calculate Arctic cloud and surface albedo feedback in CESM1 using standard methods described here. All feedback are calculated between the present-day (2006–2015) and future 10-year periods (2020–2029, 2030–2039, etc.) within the intermittent mask using monthly-mean model output. All feedback are normalized by the global annual mean surface temperature increase for each 10-year period. We use the radiative kernel method (Soden et al., 2008) with kernels developed specifically for CESM1 (Pendergrass et al., 2018) to calculate longwave cloud feedback. We use the kernel method for longwave cloud feedback, but not for shortwave cloud feedback. The radiative kernel method underestimates shortwave feedback across the sea ice edge (Shell et al., 2008). We use the approximate partial radiative perturbation method (Taylor et al., 2007) to assess shortwave feedback due to clouds and surface albedo. Approximate partial radiative perturbation is a reasonable and computationally inexpensive method of approximating the strength of the shortwave cloud feedback by decomposing how changes in cloud properties and surface albedo properties affect top-of-atmosphere shortwave flux. The approximate partial radiative perturbation method was only developed for shortwave feedback and has been used in numerous polar studies (e.g., Ceppi et al., 2014; Frey et al., 2017) to assess shortwave feedback in response to both cloud and surface albedo changes.

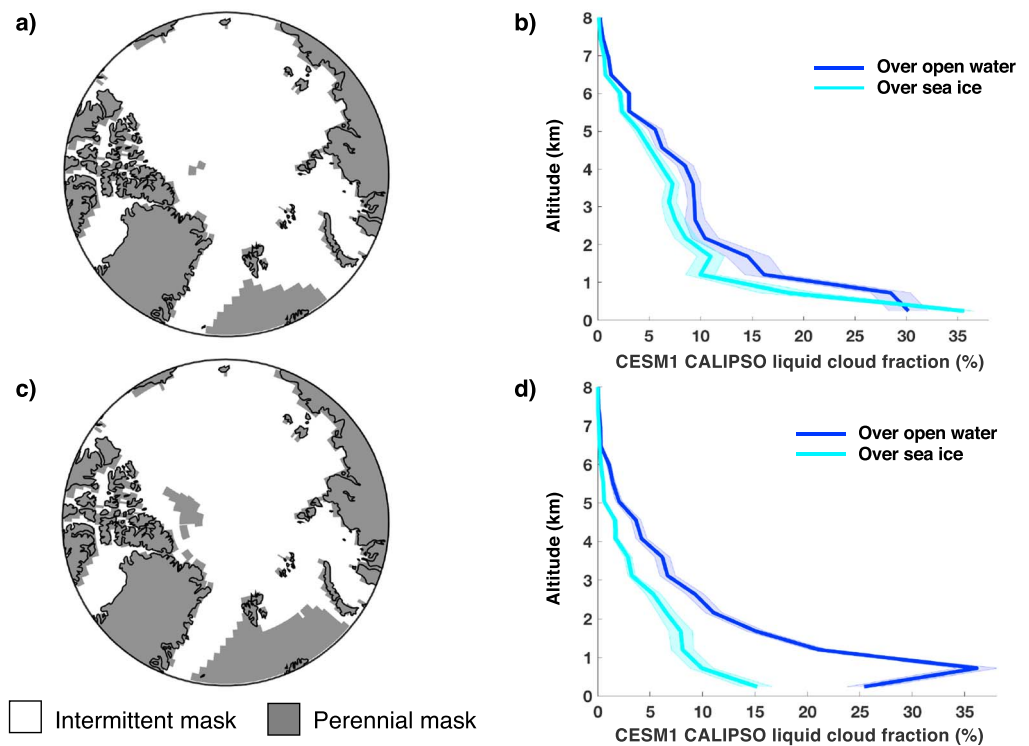


Figure 1. CESM1 CALIPSO 2006–2015 (a) summer surface masks, (b) mean summer liquid cloud fraction profiles over sea ice (sea ice concentration > 80%) and over open water (sea ice concentration < 15%), (c) fall surface masks, and (d) mean fall liquid cloud fraction profiles over sea ice and over open water within the intermittent mask. The shaded regions are one standard deviation from the mean.

3. Results

3.1. Evaluation of Present-Day Cloud-Sea Ice Relationships in CESM1 Using Observations

We begin by evaluating modeled present-day cloud-sea ice relationships in CESM1. We find that CESM1 reproduces the observed cloud response to sea ice variability both in the summer and in the fall. Within the summertime intermittent mask (Figure 1a), present-day liquid-containing cloud profiles are very similar over open water (sea ice concentration < 15%) and over sea ice (sea ice concentration > 80%; Figure 1b). In other words, the present-day summer cloud response to sea ice variability in CESM1 is very small. The lack of a cloud response to present-day sea ice variability in CESM1 during summer (Figures 1a and 1b) matches CALIPSO observations analyzed using the same methods (Morrison et al., 2018, Figure 2). In contrast, there are more liquid clouds over open water than over sea ice in the fall intermittent mask (Figures 1c and 1d). CESM1 has a present-day fall cloud response to sea ice variability, which is consistent with CALIPSO observations analyzed with the same methods (Morrison et al., 2018, Figure 6). Due to the time scales involved, the difference in clouds over open water and over sea ice results from the cloud response to sea ice cover changes and not the sea ice response to cloud changes. While clouds can respond quickly to sea ice cover changes on subdaily time scales, sea ice cover responds more slowly and is unlikely to respond to cloud changes on subdaily time scales.

We next evaluate if CESM1 replicates the observed cloud response to sea ice variability for the right reasons. In other words, we assess if the modeled cloud-sea ice relationships result from physical mechanisms that are consistent with our understanding of observed Arctic cloud-sea ice relationships. We find that the simulated cloud response to sea ice variability (Figure 1) is controlled by physical mechanisms consistent with observations and theory (Figure 2). Specifically, the physical mechanisms controlling the observed seasonal difference in cloud response to sea ice variability are seasonal differences in turbulent fluxes from the ocean to the atmosphere (Boisvert & Stroeve, 2015; Kay & Gettelman, 2009; Morrison et al., 2018). There is a strong seasonal difference in turbulent heat fluxes from the ocean to the atmosphere in the present-day CESM1:

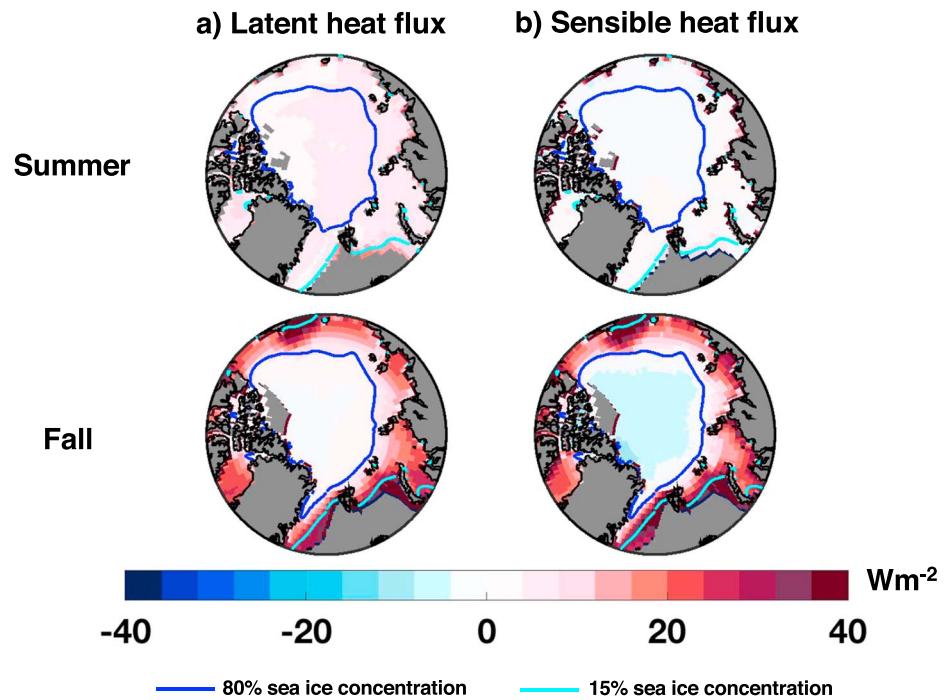


Figure 2. CESM1 2006–2015 mean summer and fall (a) latent heat fluxes and (b) sensible heat fluxes within the intermittent mask. The mean summer latent heat flux over open water (sea ice) is 7.5 Wm^{-2} (4.6 W^{-2}), and the mean summer sensible heat flux over open water (sea ice) is 3.5 Wm^{-2} (-1.3 Wm^{-2}). The mean fall latent heat flux over open water (sea ice) is 27.9 Wm^{-2} (2.1 Wm^{-2}), and the mean fall sensible heat flux over open water (sea ice) is 29.5 Wm^{-2} (1.0 Wm^{-2}). The dark blue line is the 80% sea ice concentration for summer and fall. The cyan line is the 15% sea ice concentration for summer and fall.

summer latent (Figure 2a) and sensible (Figure 2b) heat fluxes are very small compared to heat fluxes during fall. Furthermore, there are larger heat fluxes from the ocean to the atmosphere over open water than over sea ice during fall, but a negligible difference in heat fluxes over open water and over sea ice during summer.

3.2. Evaluation of the CESM1 Present-Day Mean State for Climate Context

To provide climate context for our analysis of cloud-sea ice relationships in CESM1, we next evaluate CESM1 simulations of Arctic clouds more generally. We begin by comparing modeled present-day opaque cloud cover with available CALIPSO lidar observations in the summer (Chepfer et al., 2010; Guzman et al., 2017). In the summer, CESM1 opaque cloud cover varies between 10% over the central Arctic Ocean and almost 80% over the North Atlantic (Figure 3a). As in summer, fall opaque cloud cover in CESM1 is largest over the North Atlantic, and decreases to less than 10% over the Beaufort and Chukchi Seas (Figure 3b). Compared to observations from the CALIPSO satellite, CESM1 does not have enough opaque clouds in the summer or the fall (Figures 3c and 3d). The largest summer opaque cloud biases are over the Barents and Kara Seas (Figure 3c). Indeed, the model struggles to represent both the amount and location of opaque clouds. As in summer, we also find insufficient opaque cloud cover in CESM1 during fall (Figure 3d). The largest biases in fall cloud cover occur around the central Arctic Ocean. Insufficient opaque cloud cover in CESM1 is consistent with previous studies that also found insufficient liquid-containing clouds in CESM1 (Kay, Bourdages, et al., 2016).

Why are there not enough opaque clouds in CESM1? Clouds are controlled by both microphysical processes and their dynamical environment (Klein & Hartmann, 1993; Morrison et al., 2012). From a microphysical perspective, CESM1 overestimates ice precipitation from Arctic clouds, leading to excessive depletion of supercooled liquid and thus insufficient opaque cloud cover (McIlhatten et al., 2017). There are biases in CESM1 Arctic synoptic regimes that influence opaque cloud biases as well. Here we show these biases by comparing summer and fall sea level pressure from 1986 to 2015 in CESM1 against ERA-Interim (ERA-I) reanalysis (Dee et al., 2011). We use a 30-year record to reduce the influence of internal climate variability on our

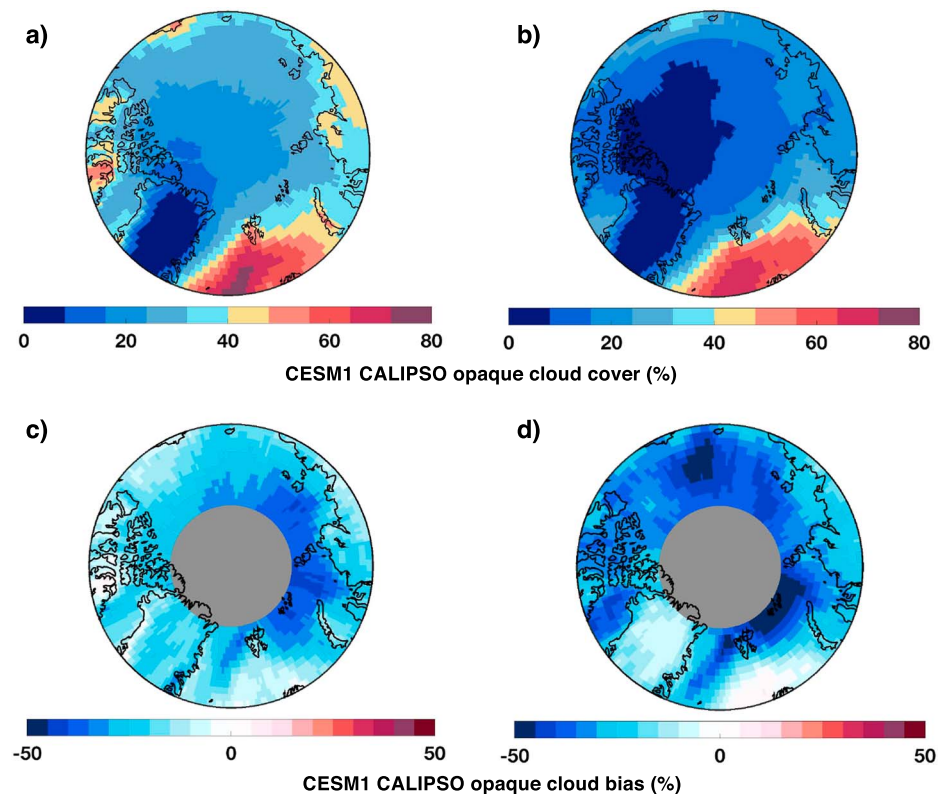


Figure 3. Mean state from 2006 to 2015 for CESM1 CALIPSO opaque cloud cover during (a) summer (JJA) and (b) fall (SON), and difference between observed and simulated CESM1 CALIPSO opaque cloud cover during (c) summer (JJA) and (d) fall (SON). CESM1 CALIPSO opaque cloud biases are calculated against CALIPSO-GOCCP observations.

model-observation comparisons. We use the ERA-I reanalysis because Arctic sea level pressure biases are within 1 hPa of observations (Wesslén et al., 2014). In the summer, the highest mean state sea level pressure in CESM1 is over Greenland and the Beaufort Sea (Figure 4a). In the fall, there is a mean state sea level pressure dipole over the Arctic Ocean, with a high-pressure center over the Chukchi-East Siberian Seas and a low-pressure center over the North Atlantic (Figure 4b). Compared to ERA-I, the CESM1 mean state sea level pressure during summer is too high (Figure 4c), possibly suppressing cloud cover. CESM1 exhibits large positive sea level pressure biases over the Barents and Kara Seas, which match the opaque cloud biases (Figure 3c). In the fall, mean state sea level pressure is too low over the Beaufort Sea but slightly too high over the Barents and Kara Seas (Figure 4d). Overall, CESM1 sea level pressure biases are smaller during fall than they are in summer.

3.3. Future Arctic Cloud-Sea Ice Relationships in CESM1: Changes and Physical Mechanisms

Acknowledging that CESM1 has important biases including insufficient opaque cloud but encouraged that CESM1 reproduces present-day observed sea ice relationships, we next evaluate future Arctic cloud-sea ice relationships and feedback simulated by CESM1. All future cloud profiles are analyzed within the present-day intermittent mask, because that is the region where sea ice extent drastically declines over the next century. Future open water within the intermittent mask is a direct result of sea ice loss. Therefore, we compare future cloud profiles over open water against present-day cloud profiles over sea ice. Comparing future clouds over open water with clouds over sea ice in the present allows us to see if clouds respond similarly to open water in the future as they do in the present. In other words, does open water have the same influence on clouds in the future as it does in the present (Figure 1)? Are clouds still coupled to the surface during fall and uncoupled from the surface during summer?

First are the summer cloud results. Open water encompasses a larger region of the Arctic Ocean during each future period (Figure 5a), growing poleward from the North Atlantic and Bering Strait. Over open water,

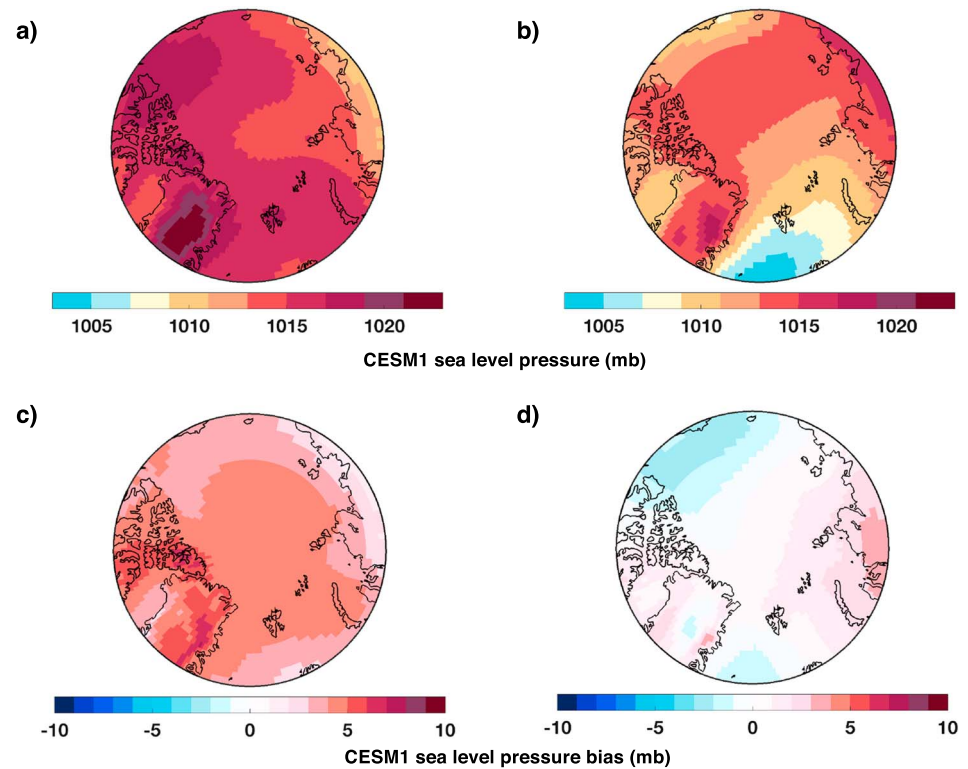


Figure 4. Same as in Figure 3 but for sea level pressure mean state in CESM1, 1986–2015. CESM1 summer and fall sea level pressure biases are calculated against ERA-Interim reanalysis.

low-level (<4 km) summer cloud fraction decreases slightly from 2006 to 2015 through the end of the twenty-first century, but changes in the summer cloud profiles over open water are very small. Indeed, open water summer cloud profiles in each future period (cyan, blue, green, and purple lines; Figure 5b) are nearly identical to the present-day summer cloud profile over sea ice (black dotted line; Figure 5b). The cloud vertical structure remains unchanged no matter the time period or surface type. Importantly, even though open water areas in the future Arctic will grow and encompass different areas than open water in the present, summer cloud fraction and structure are unaffected by larger regions of the Arctic Ocean becoming open water. Summer clouds are unaffected by open water no matter where the open water is. Together, the very small cloud fraction change and the lack of vertical structure change over open water suggest that there is no summer cloud response to sea ice loss in the future Arctic, just as there is no response to summer sea ice variability in the present. No cloud-sea ice feedback exists in the present nor is predicted to emerge in the future.

Next we assess fall cloud results. By the end of the twenty-first century, the Arctic Ocean is almost completely sea ice-free (Figure 5c). Fall cloud fraction over the open water in all future time periods (cyan, blue, green, and purple lines; Figure 5d) is always larger than the present-day fall cloud fraction over sea ice (black dotted line; Figure 5d). In contrast to the summer (Figure 5b), CESM1 predicts changes to future fall vertical cloud structure over open water. The most striking change is that the boundary layer deepens over open water at the end of the twenty-first century. Sea ice loss, which results in most of the fall Arctic Ocean being open water by the end of the century, changes the vertical structure of fall clouds. Between 2006–2015 and 2080–2099, liquid cloud fraction at ~2 km increases by nearly 7%, and decreases by nearly 9% below 1 km over open water. The cloud fraction decrease is likely due to lidar attenuation. Since the simulated lidar is attenuated through optically thick clouds in CESM1, a reduction in the maximum fall cloud fraction below 1 km over time may indicate more *opaque* cloud just above 1 km in the future. We emphasize that even with simulated lidar attenuation, the future cloud fraction over open water is still always larger than the cloud fraction over present-day sea ice. In summary, our results suggest that present-day cloud-sea ice relationships are good analogues for future cloud-sea ice relationships.

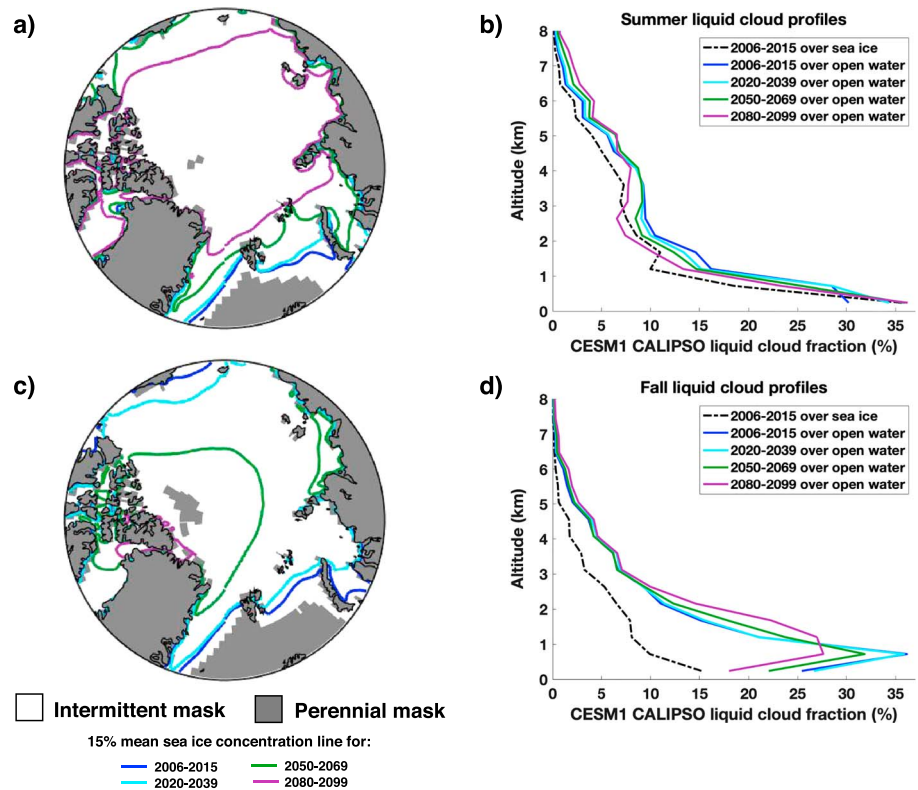


Figure 5. The cloud response to increased future open water during summer and fall: (a) summer open water extent for 2006–2015, 2020–2039, 2050–2069, and 2080–2099; (b) summer liquid cloud profiles over sea ice for 2006–2015 and over open water for 2006–2015, 2020–2039, 2050–2069, and 2080–2099; (c) fall open water extent for 2006–2015, 2020–2039, 2050–2069, and 2080–2099; and (d) fall liquid cloud profiles over sea ice for 2006–2015 and over open water for 2006–2015, 2020–2039, 2050–2069, and 2080–2099. All cloud profiles are from the present-day intermittent mask (shown in white in (a) and (c)). The future open water extent is the mean 15% sea ice concentration line for each time period. Over open water, the mean summer sea level pressure from 2006–2015 (2091–2095) is 1,017 mb (1,016 mb) and the mean summer near-surface static stability from 2006–2015 (2091–2095) is 4.8 K (7.9 K). Over open water, the mean fall sea level pressure from 2006 to 2015 (2091–2095) is 1,012 mb (1,013 mb), and the mean fall near-surface static stability from 2006 to 2015 (2091–2095) is 4.8 K (4.3 K).

As in observations, seasonal differences in heat fluxes explain the seasonal difference in future summer and fall cloud response to sea ice loss in CESM1. Changes in summer latent (Figure 6a) and sensible (Figure 6b) heat fluxes are negligible between 2006–2015 and 2080–2099. There is no spatial correlation between summer heat flux changes and the sea ice loss edge (green line) in CESM1. But during the fall, latent (Figure 6a) and sensible (Figure 6b) heat fluxes increase by up to 30 Wm^2 between 2006–2015 and 2080–2099. Changes in sensible heat fluxes closely follow the sea ice loss edge in the fall months, but changes in latent heat fluxes are less constrained to the sea ice loss edge in September. Latent heat flux changes are less constrained to the sea ice loss edge in September because it is a transition month: early September behaves like the summer, but late September behaves like the fall. The atmosphere and ocean are decoupled early in the month, but air-sea coupling grows stronger as the Sun sets and the atmosphere cools.

While changes in cloud occurrence are interesting and important, cloud influence on radiation depends also on cloud properties. Thus, we next assess twenty-first century changes in two radiatively important cloud properties: cloud liquid water path and cloud shortwave optical depth. Even though mean heat flux changes are negligible in the summer (Figure 6), monthly mean liquid water path does increase from June to November in 2080–2099 relative to 2006–2015 (Figure 7a). Shortwave optical depth increases in all months between 2006–2015 and 2080–2099 (Figure 7b). By 2080–2099, September has the largest optical depth value of 7.5. The largest optical depth percent increase, however, is in November: an $\sim 157\%$ increase between 2006–2015 and 2080–2099. From September to November, all optical depth percent increases between 2006–2015 and 2080–2099 are at least 100%. Importantly, the increases in fall optical depth

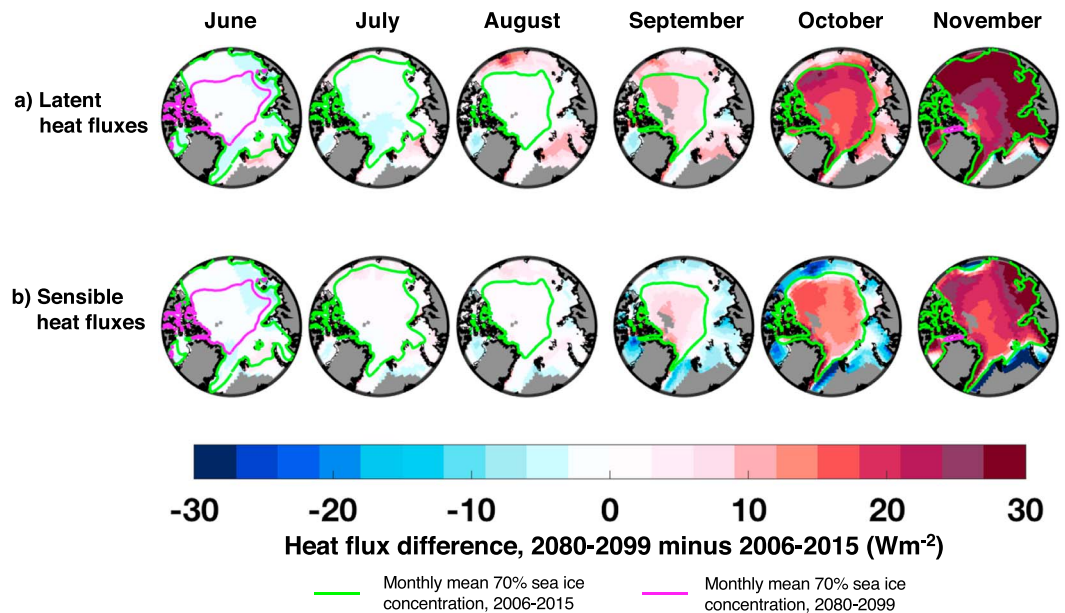


Figure 6. Difference in CESM1 monthly mean (a) latent and (b) sensible heat fluxes between 2006–2015 and 2080–2099. The green (pink) line is the monthly mean 70% sea ice concentration for 2006–2015 (2080–2099). From July to November, the mean sea ice concentration never reaches 70% in 2080–2099. The green line can therefore be considered the “sea ice loss edge”—that is, where sea ice used to be in the present day but is gone by the end of the twenty-first century.

show that fall clouds transition from being optically thin in the present day (optical depth < 3) to optically thick in the future (Chepfer et al., 2013). Once clouds become optically thick, direct solar radiation, and lidar pulses as we are simulating here, no longer reach the surface. Since there is still Sun in the Arctic from September through early November, increasing cloud optical depth still strengthens clouds’ shortwave effect in the fall. In comparison to the fall, there are very small changes to radiatively important summer cloud properties in CESM1 from the present (2006–2015) to the far future (2080–2099).

As we have shown in present-day variability (Figures 1b and 1d) and in response to future sea ice loss (Figure 5), sea ice can affect clouds by modifying turbulent fluxes from the ocean to the atmosphere. The modeling results presented thus far show no impact of summer sea ice loss on clouds, a result that is consistent with observations. But it has long been known that there is a seasonal delay in the impact of summer sea ice loss on the atmosphere (Abe et al., 2016; Curry et al., 1995; Manabe & Stouffer, 1980; Sorteberg et al., 2007). Therefore, does summer sea ice loss have a delayed impact on fall clouds? If so, what are the mechanisms controlling the impact of summer ice loss on fall clouds? Present-day observations suggest the fall atmosphere destabilizes in direct response to a longer summer melt season. Atmospheric instability during fall leads to more clouds in the Arctic, so we next investigate the chain of events that lead summer sea ice loss to increase near-surface static instability and cloud formation during fall in CESM1. Here we define near-surface static stability as the difference in potential temperature between 925 and 1,000 mb (following Kay & Gettelman, 2009). As summer sea ice disappears more shortwave is absorbed by the open ocean (Figure 8a) and the heat content of the CESM1 ocean mixed-layer increases (Figure 8b). The longer the open water season is, the more time the surface ocean has to absorb heat from incoming sunlight. By the end of the twenty-first century, mixed-layer ocean heat content is positive in all months, but highest in late summer (Figure 8b). As the Sun sets in the fall, accumulated surface ocean heat is released into the atmosphere. The largest combined latent and sensible heat fluxes occur when the ocean is still ice-free but the air-sea temperature gradient is largest, both of which occur in November in 2080–2099. Total heat flux change from 2006–2015 to 2080–2099 is smallest in July, and actually decreases over the same time period in June (Figure 8c). Releasing accumulated surface ocean heat into the atmosphere during fall weakens the near-surface atmospheric stability (Figure 8d). As ocean heat content increases in November from 2006–2015 to 2080–2099, near-surface static stability decreases by 87% over the same period. But despite a large increase in summer ocean heat content, there is very little corresponding change in summer near-surface static

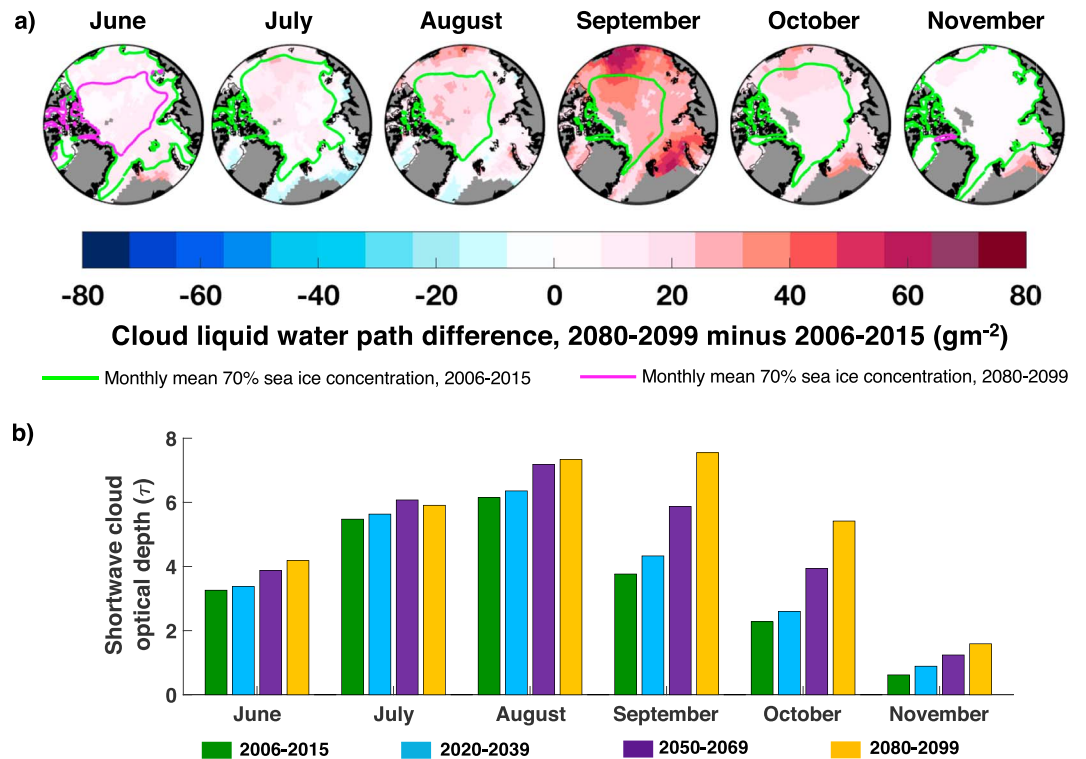


Figure 7. (a) Difference in CESM1 monthly cloud liquid water path between 2006–2015 and 2080–2099. The green (pink) line is the 70% monthly mean sea ice concentration for 2006–2015 (2080–2099). (b) Time series of monthly mean summer (JJA) and fall (SON) CESM1 shortwave cloud optical depth within the intermittent mask for 2006–2015 (green), 2020–2039 (blue), 2050–2069 (purple), and 2080–2099 (yellow).

stability. In sum, summer sea ice loss has little impact on the summer atmosphere but does indeed have a delayed atmospheric impact which is felt during fall.

In the results presented thus far, we have focused on summer and fall clouds because observed sea ice loss is largest in these seasons and thus CESM1 cloud-sea ice relationships can be most directly evaluated using observations in these seasons. But what about clouds in the winter and spring? The lidar simulator in CESM1 allows us to see what CALIPSO-GOCCP would observe in all future months including winter and spring. Through physical intuition, we expect the winter and spring cloud response to sea ice loss to be very similar to the fall cloud response to sea ice loss (Figure 5d). In other words, loss of sea ice increases strong air-sea coupling and cloud cover. In contrast to the fall, the Arctic still has sea ice during winter (December-January-February) and spring (March-April-May) by the end of the twenty-first century in CESM1, but open water areas within the seasonal intermittent masks consistently grow over time (Figures 9a and 9c). In the winter (Figure 9b) and spring (Figure 9d), liquid cloud structure over open water within the seasonal intermittent masks remains relatively unchanged into the future in CESM1. The cloud vertical fraction increases steadily over time, however, as more open water exists in the winter. The maximum winter cloud fraction nearly doubles between 2006–2015 and 2080–2099. In the spring, the maximum cloud fraction also increases over time, although the change is smaller than in the winter.

We next analyze changes in cloud cover to assess if the cloud response to sea ice loss controls the total cloud response to increased greenhouse gases. Consistent with the cloud fraction profiles (Figure 5), we find no future total or opaque summer cloud cover response to sea ice loss within the annual intermittent mask but more nonsummer season clouds over open water (Figure 10). Spatially, the nonsummer cloud response is strongly correlated with the sea ice loss edge (green line). By 2080–2099, the smallest total (Figure 10a) and opaque (Figure 10b) cloud increases are in the early summer (May–June), and the largest total and opaque cloud increases are in the late fall (November–December). Total cloud cover in the nonsummer seasons increases by up to 66% relative to 2006–2015 (Figure 10). Cloud increases have little spatial correlation

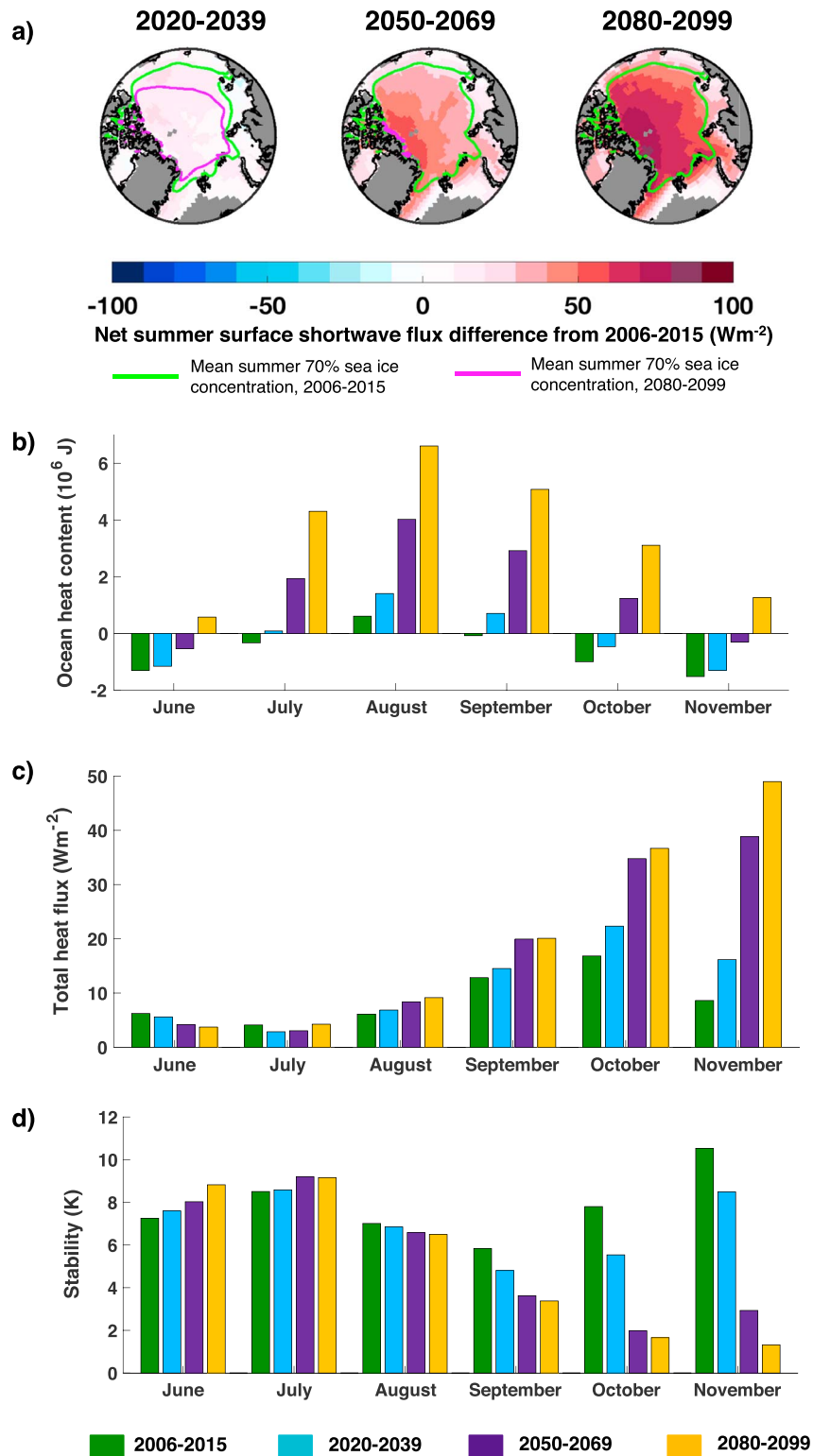


Figure 8. (a) Difference in CESM1 all-sky net surface shortwave fluxes between 2006–2015 and 2020–2039, 2050–2069, and 2080–2099. (b) Time series of monthly mean summer (JJA) and fall (SON) CESM1 mixed-layer ocean heat content within the intermittent mask for 2006–2015 (green), 2020–2039 (blue), 2050–2069 (purple), and 2080–2099 (yellow). Ocean heat content is calculated with a temperature gradient between the surface and the bottom of the mixed layer, so heat content is negative when the surface is colder than the bottom of the mixed layer (McDougall & Barker, 2011). (c) Time series of CESM1 monthly mean total (combined latent and sensible) heat flux from the ocean to the atmosphere within the intermittent mask. (d) Time series of CESM1 monthly mean near-surface static stability ($\Theta_{925 \text{ mb}} - \Theta_{1,000 \text{ mb}}$) within the intermittent mask.

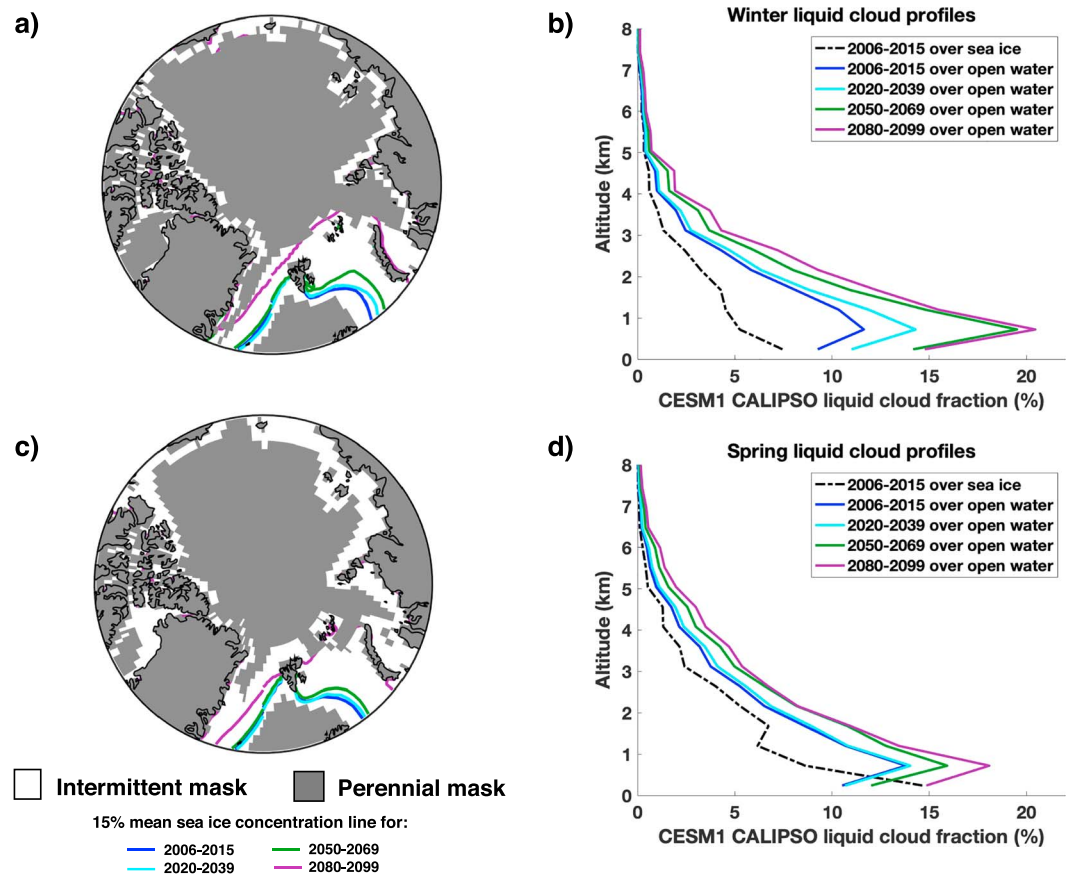


Figure 9. The cloud response to increased future open water during winter and spring: (a) winter open water extent for 2006–2015, 2020–2039, 2050–2069, and 2080–2099; (b) winter liquid cloud profiles over sea ice for 2006–2015 and over open water for 2006–2015, 2020–2039, 2050–2069, and 2080–2099; (c) spring open water extent for 2006–2015, 2020–2039, 2050–2069, and 2080–2099; and (d) spring liquid cloud profiles over sea ice for 2006–2015 and over open water for 2006–2015, 2020–2039, 2050–2069, and 2080–2099. All cloud profiles are from the present-day intermittent mask (shown in white in (a) and (c)). The future open water extent is the mean 15% sea ice concentration line for each time period.

with the sea ice loss edge (green line) in summer, but increasingly follow the sea ice loss edge from September to February (Figure 10a). Indeed, from September to February there are only small cloud changes *outside* the sea ice loss edge, indicating that fall and winter cloud changes occur almost entirely over newly open water from 2080 to 2099. Opaque cloud cover increases very little from May to August compared to September–February (Figure 10b). In the early fall (September–October), opaque cloud cover increases are not constrained to the sea ice loss edge the way that total cloud cover increases are. The largest changes in nonsummer opaque cloud cover are on the margins of the Arctic Ocean, which is where present-day fall opaque cloud cover is largest (Figure 4a). Increasing fall opaque cloud cover over time means that the lidar is also attenuated more over time, leading to the decreased maximum fall cloud fraction in Figure 5d.

The fall, winter, and spring exhibit similar cloud responses to sea ice loss, but the fall cloud changes are more pronounced than the winter or spring cloud changes. For example, total and opaque cloud cover increases are largest in the late fall (Figure 10); fall is the only season when vertical cloud structure changes over open water (Figures 5 and 9). Why is the cloud response to sea ice loss different in the fall? The answer is connected to the seasonal delay in the impact of summer sea ice loss on the atmosphere. As the Arctic warms and sea ice disappears, the sea ice melt date occurs earlier in the spring and the freezeup date occurs later in the fall. A later freezeup date means that there is more time in the fall for accumulated ocean heat to be released into the atmosphere. Accumulated ocean heat is released into the atmosphere during fall and early winter, and by the late winter and spring the ocean has lost much of its accumulated heat. As the melt season lengthens, the

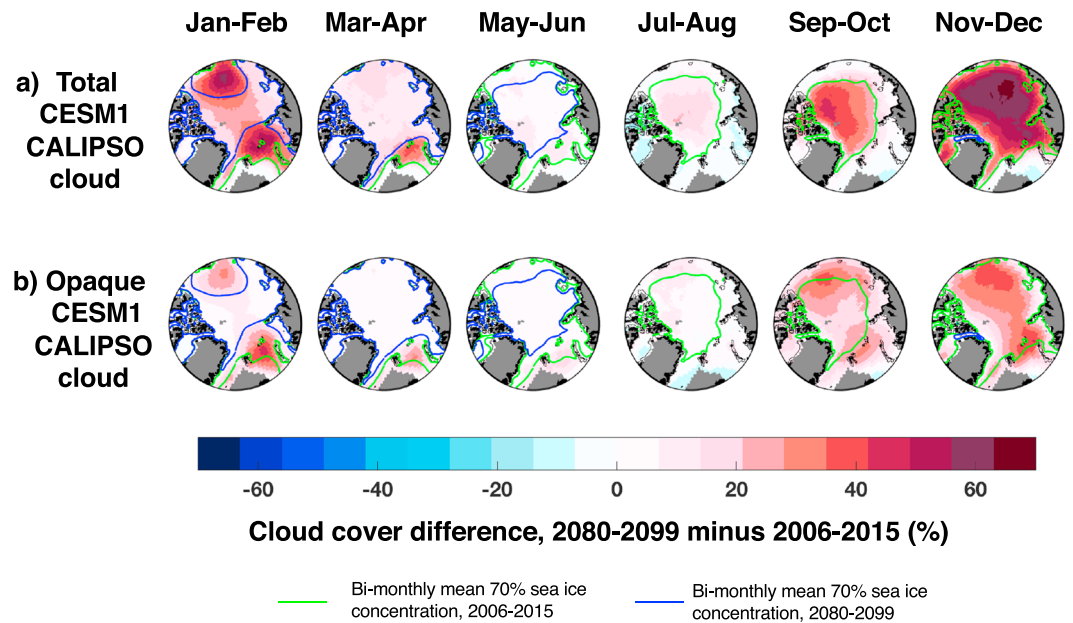


Figure 10. Difference in CSM1 CALIPSO bimonthly mean (a) total and (b) optically opaque cloud cover between 2006–2015 and 2080–2099. The green (blue) line is the 70% bimonthly mean sea ice concentration for 2006–2015 (2080–2099). The green line is the “sea ice loss edge”—that is, where sea ice used to be in the present day but is gone by the end of the twenty-first century.

ocean has more time to accumulate heat that will then be released into the fall atmosphere. Over time, more accumulated ocean heat is released into the atmosphere in all nonsummer seasons, but the change is smallest in the spring because by the spring the ocean has already lost most of its heat to the atmosphere. This small increase in heat flux from the ocean to the atmosphere in the spring translates into the smallest nonsummer cloud fraction increase (Figures 5d and 9).

3.4. Cloud and Surface Albedo Feedback in CSM1

We have identified year-round cloud responses to sea ice loss, but what is the sign and strength of the year-round cloud feedback as clouds change in response to sea ice loss? In other words, what is the role of sea ice loss in affecting future cloud feedback in the Arctic? We start to answer these questions by showing the evolution of annual mean longwave, shortwave, and total cloud feedback and the surface albedo feedback as a function of annual mean global warming (Figure 11). The surface albedo feedback (black line) strengthens rapidly until global mean warming reaches ~ 1.5 K, which occurs in the 2040s. After global mean warming exceeds 1.5 K, the surface albedo feedback weakens over time from 13 to $8 \text{ Wm}^2/\text{K}^1$. The surface albedo feedback eventually weakens because once the Arctic becomes sea ice-free in September by the 2060s in our simulation (sea ice extent $< 1 \times 10^6 \text{ km}^2$), the surface albedo difference between the present and future climatic states remains roughly constant. The surface albedo does continue to decrease slightly until the sea ice is entirely gone (September Arctic sea ice concentration $< 1\%$ everywhere), but the rate of surface albedo change is very small. Global mean temperature increases linearly through 2100 so temperature changes outpace surface albedo changes. Since the growth rate of the normalizing factor (global annual mean warming; see section 2.3) is faster than the rate of surface albedo change, the surface albedo feedback weakens after the 2040s (Figure 11). Even though the surface albedo feedback weakens at the end of the twenty-first century, it is still an order of magnitude larger than the cloud radiative feedback. The longwave cloud feedback (red line) is positive through the end of the twenty-first century but decreases slightly over time. The shortwave cloud feedback (blue line) is slightly positive in the 2020s but becomes negative as global mean warming increases above 0.5 K. Overall, the net cloud feedback (gray line) is very small. For example, during the 2090s when global warming has reached 4 K, the net Arctic cloud feedback is $0.4 \text{ Wm}^2/\text{K}$. While small, the net Arctic cloud feedback in CSM1 oscillates between positive and slightly negative as it is dominated by either the positive longwave cloud feedback or the negative shortwave cloud feedback.

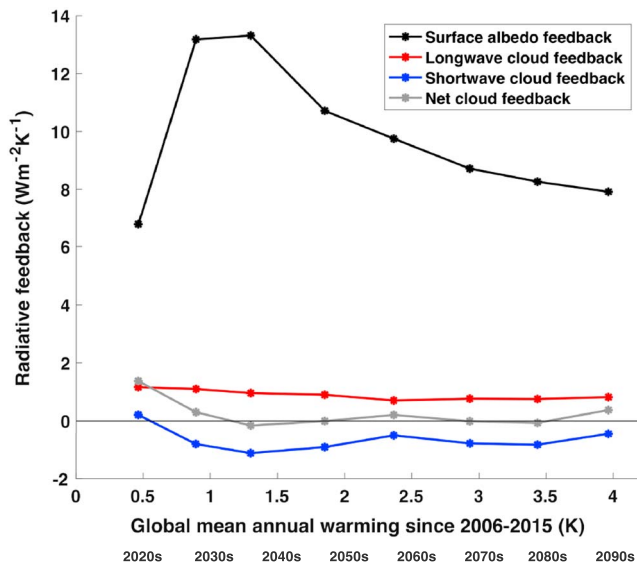


Figure 11. Time series of surface albedo, longwave cloud, shortwave cloud, and net cloud feedback versus global annual mean warming from 2006–2015 through 2099. The time periods corresponding to each temperature increase are shown at the bottom of the figure.

Given the strong seasonality of cloud-sea ice relationships in the Arctic, we next investigate seasonal changes in longwave cloud feedback (Figure 12). While a positive longwave cloud radiative feedback occurs in all seasons (Figure 12a), winter is the only season when the longwave cloud feedback strengthens over time. The longwave feedback decreases in all other seasons, although the change is very small in the fall. The summer longwave cloud feedback weakens the most: from 1.7 Wm^2/K in the 2020s to 0.3 Wm^2/K in the 2090s (Figure 12a). The weakening summer longwave feedback therefore counteracts some of the nonsummer signal when the longwave feedback is averaged over the whole year (Figure 11).

Seasonal changes in longwave cloud radiative effect (Figure 12b) are consistent with our previous results of increasing cloud opacity and cover in the nonsummer seasons (Figures 7, 9, and 10). Compared to 2006–2015, the longwave cloud radiative effect strengthens in all nonsummer seasons and remains nearly constant in the summer (Figure 12b). Connecting longwave cloud radiative effect to longwave cloud feedback, winter is the only season where longwave cloud feedback increases over time because it is the only season where the longwave flux due to cloud changes, which includes the contribution from longwave cloud radiative effect, grows faster than global mean temperature increases. In other words, the rate of increase for winter longwave cloud radiative effect is faster than the rate of increase for global mean temperature, which means that the winter

longwave cloud feedback grows more positive over time as well. Fall longwave cloud feedback stays roughly constant because the change in longwave flux due to fall cloud changes increases more slowly than global temperatures do. Spring longwave cloud feedback decreases over time because the spring longwave cloud radiative effect does not increase as fast as global temperatures do. The rate of change for spring longwave

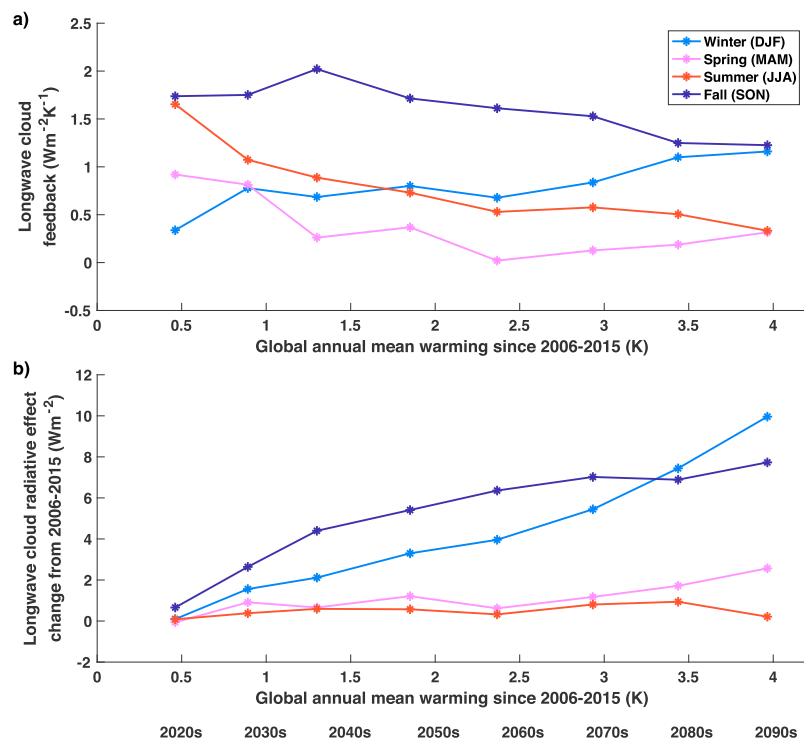


Figure 12. (a) Time series of winter, spring, summer, and fall longwave cloud feedback. (b) Change in winter, spring, summer, and fall longwave cloud radiative effect since 2006–2015. The time periods corresponding to each temperature increase are shown at the bottom of the figure.

cloud radiative effect is slower than the rate of change for global mean temperature. The summer longwave cloud radiative effect stays constant in the future, consistent with Figures 7 and 10 that show negligible changes to summer radiative properties and cloud cover. Using Arctic mean warming as the normalizing factor instead of global mean warming produces even weaker longwave cloud radiative feedback (not shown) because Arctic temperature rises faster than global mean temperature.

4. Discussion

One of the most interesting and important results from this study is that the summer cloud response to present-day sea ice variability is consistent with future summer cloud-sea ice feedback. Using a model that reproduces the lack of an observed present-day summer cloud response to present-day summer sea ice variability, we find no summer cloud-sea ice feedback emerges as the Arctic becomes seasonally sea ice-free. In other words, the summer cloud-sea ice relationship is not changing as the climate warms. The surface is not a strong control on summer clouds in the present or in the future. Thus, the present-day summer cloud response to present-day summer sea ice variability helps predict future summer Arctic sea ice-cloud relationships. These findings are consistent with physical intuition for an increasingly stable future Arctic summer atmospheric boundary layer. In the present-day summer, a small air-sea temperature gradient stabilizes the lower atmosphere and suppresses fluxes from the open ocean to the air. Given the specific heat capacity difference of air and water, as the Arctic warms the atmosphere warms faster than the ocean, even when the ocean is ice-free. Therefore, summer near-surface static stability will remain the same or increase as the Arctic warms. A stable summer atmosphere suppresses fluxes from the ocean to the atmosphere in the present day *and* in the future. The surface is not a strong control on summer clouds because the small air-sea temperature gradient that currently exists still exists in the future. Summer clouds are controlled by atmospheric circulation in both the present and the future, although fully identifying the dominant controls on summer clouds is outside the scope of this paper.

Another interesting and important result from this study is that observed cloud-sea ice relationships also help explain future Arctic cloud-sea ice feedback during nonsummer months. Why? As in the summer, future fall cloud-sea ice relationships result from air-sea temperature gradients. When the Sun sets in the fall, the atmosphere cools down faster than the ocean. As a result, more latent and sensible heat is released from the open ocean to the cooling fall atmosphere (as has been shown in many studies including Deser et al. (2010), Manabe & Stouffer (1980), and Taylor et al. (2018)). Increasing latent and sensible heat fluxes promote fall cloud formation over open water. As the freezeup onset date moves later in the year, there will be more open water during fall, sea ice will be thinner in winter, and melt onset will occur earlier in the spring. Summer sea ice loss does not affect summer clouds but there is a lag between summer sea ice reduction and increased cloudiness in the fall. Importantly for cloud feedback resulting from sea ice loss, more open water during the fall, winter, and spring means more clouds during these seasons because of the large heat fluxes from open water to the atmosphere.

Connecting our analysis of cloud-sea ice relationships into a broader climate context, we find evidence for a weak positive Arctic cloud-sea ice feedback that arises from increases in nonsummer clouds and their impact on longwave radiation. A positive annual mean net cloud-sea ice feedback indicates that clouds enhance warming of the Arctic surface in response to increased greenhouse gases (Goosse et al., 2018). While our results suggest the Arctic cloud-sea ice feedback is positive and is a large contributor to the total Arctic cloud feedback, the Arctic cloud feedback we found are relatively weak compared to the surface albedo feedback. Arctic cloud feedback are an order of magnitude smaller than the surface albedo feedback, consistent with previous analysis of climate model feedback (e.g., Pithan & Mauritsen, 2014). Nevertheless, Arctic cloud-sea ice relationships and feedback do affect Arctic climate futures. Because of a positive longwave cloud-sea ice feedback and strengthening longwave cloud radiative effect, especially during the fall and winter, clouds likely enhance Arctic warming in the future. Since predicted summer cloud changes in response to sea ice loss are very small, we found no evidence that future summer cloud-sea ice feedback will affect summer Arctic sea ice loss.

While we are confident in our assessed positive sign for the Arctic cloud-sea ice feedback, the magnitude of the positive Arctic cloud-sea ice feedback may be underestimated by the model used in this study. Our assessment of the sign of the Arctic cloud-sea ice feedback is informed by new rigorous evaluation of the

cloud-sea ice relationships and cloud opacity in CESM1 using spaceborne lidar observations. In contrast to the sign, we interpret the magnitude of our assessed Arctic cloud-sea ice feedback with caution. Indeed, we suspect that the underestimation of mean state opaque clouds in CESM1 may lead to an underestimation of the magnitude of Arctic cloud feedback in CESM1 including the positive cloud-sea ice feedback associated with sea ice loss. The longwave cloud feedback may be more positive than predicted by CESM1, but the shortwave cloud feedback may be more negative than predicted. The strength of the longwave cloud-sea ice feedback would likely increase faster than the strength of the shortwave cloud feedback, since predicted cloud fraction and opacity increases during the nonsummer seasons are much larger than summer cloud changes. In that case, we are likely underestimating the strength of the positive annual total cloud feedback. CESM1 is not alone in its underestimation of opaque clouds, which are primarily liquid clouds. Indeed, many models underestimate observed liquid clouds and thus may also underestimate the positive cloud-sea ice feedback (e.g., Klein et al., 2013).

Looking toward future analysis of cloud-sea ice relationships and Arctic cloud feedback in models, we wish to emphasize that the results obtained in this study cannot be obtained from the standard climate model output. That is, our results cannot be obtained from output typically provided by intermodel comparison projects: monthly mean output provided in CMIP5 or outputs with specific relevance for assessing cloud feedback requested for CMIP6 (Webb et al., 2017). First, creating the intermittent mask requires daily sea ice concentration output. Second, we also require daily sea ice and cloud output to get as close as possible to an instantaneous snapshot of the cloud response to variations in sea ice cover. On longer time scales the sea ice could be responding to variations in cloud cover instead of clouds responding to variations in sea ice cover. The use of monthly mean output averages clouds over different atmospheric and sea ice regimes and makes it harder to isolate a cloud response just to sea ice variability. Third, our results require a lidar simulator to be used when comparing model clouds with satellite observations. We needed a lidar simulator specifically because lidars are “surface-blind” sensors and are the best tools for detecting clouds over sea ice. Using the lidar simulator within COSP to assess both the present *and* future cloud response to sea ice was necessary because cloud cover from CESM1 and from the CALIPSO satellite are defined differently. It is advantageous to use the same definition for “cloud” across all time periods. For a process-based understanding of cloud-sea ice relationships in a model, we needed COSP and the cloud opacity diagnostics to evaluate changes in radiatively important cloud properties, that is, opaque clouds that are interacting with shortwave radiation. The methods used here are novel, and provide a new and robust procedure for assessing modeled cloud-sea ice relationships and giving guidance for the observability of future cloud changes arising from sea ice loss.

Acknowledgments

This work was supported by NASA grant 15-CCST15-0025, the Air Force Institute of Technology, the Centre National d'Études Spatiales (CNES), and by the Université Pierre et Marie Curie. A.L.M. was also partially supported by the Chateaubriand Fellowship of the Office for Science & Technology of the Embassy of France in the United States; A.L.M. and J.E.K. thank École Polytechnique for its hospitality during part of this study. The CALIPSO-GOCCPv3.1.2 cloud and sea ice data were uploaded from the ClimServ computing center (<http://climserv.ipsl.polytechnique.fr/>). ERA-Interim sea level pressure and potential temperature data are available at <http://apps.ecmwf.int/datasets/data/interim-full-mode/lev-type=sfc/>. Netcdf files of monthly mean variables from CESM1-COSP1.4 model output are stored on the Open Science Framework (<https://osf.io/5ftq2/>). All CESM1-COSP1.4 data were produced using supercomputing resources provided by NSF/CISL/Cheyenne. The CESM project is supported by the National Science Foundation and the Office of Science (BER) of the U.S. Department of Energy. The authors thank A. Gettelman and three anonymous reviewers for their insightful and constructive comments on the manuscript. The views expressed in this article are those of the authors and do not reflect the official policy or position of the U.S. Air Force, Department of Defense, the U.S. Government, or the French Government. We declare no competing financial interests.

5. Summary

This study uses a fully-coupled climate model (CESM1) with a lidar simulator and cloud opacity diagnostic to assess present-day and future changes in Arctic cloud sea ice relationships and feedback. CESM1 is an appropriate tool to use because it can replicate the observed cloud response to sea ice variability. Future Arctic cloud-sea ice relationships are very similar to present-day relationships, indicating that observed variability is a good analogue for the future ice-free Arctic climate. Over the twenty-first century, CESM1 predicts negligible changes in summertime cloud fraction and vertical structure due to negligible changes in summer ocean heat fluxes. Any future summer cloud changes in CESM1 are uncorrelated with the sea ice loss edge. CESM1 predicts large increases in fall cloud fraction and boundary layer height, as well as in radiatively important properties like liquid water path and opaque cloud fraction. Future winter and spring low-level cloud fraction increase as well. Since cloud cover increases in all nonsummer seasons in response to sea ice loss, the positive longwave cloud radiative effect also increases in the nonsummer seasons. The strong nonsummer cloud response to sea ice loss leads to a positive cloud-sea ice feedback, which will accelerate the rate of sea ice loss. Since summer clouds do not respond to sea ice loss, no negative cloud-sea ice feedback exists. Summer cloud-sea ice feedback will not slow the rate of Arctic sea ice loss.

References

- Abe, M., Nozawa, T., Ogura, T., & Takata, K. (2016). Effect of retreating sea ice on Arctic cloud cover in simulated recent global warming. *Atmospheric Chemistry and Physics*, 16(22), 14,343–14,356. <https://doi.org/10.5194/acp-16-14343-2016>
- Bailey, D., Holland, M., Hunke, E., Lipscomb, B., Briegleb, B., Bitz, C., & Schramm, J. (2011). Community Ice Code (CICE) user's guide version 4.0 released with CCSM 4.0. Technical Report, National Center for Atmospheric Research, Boulder, Colorado, 24 pp.

- Barnhart, K. R., Miller, C. R., Overeem, I., & Kay, J. E. (2016). Mapping the future expansion of Arctic open water. *Nature Climate Change*, 6(3), 280–285. <https://doi.org/10.1038/nclimate2848>
- Bindoff, N. L., Stott, P. A., AchutaRao, K. M., Allen, M. R., Gillett, N., Gutzler, D., et al. (2013). Chapter 10: Detection and attribution of climate change: From global to regional. In T. F. Stocker, et al. (Eds.), *Climate Change 2013: The Physical Science Basis. Contribution of Working Group I to the Fifth Assessment Report of the Intergovernmental Panel on Climate Change* (pp. 867–952). Cambridge, United Kingdom and New York, NY, USA: Cambridge University Press.
- Blackport, R., & Kushner, P. J. (2017). Isolating the atmospheric circulation response to Arctic sea ice loss in the coupled climate system. *Journal of Climate*, 30(6), 2163–2185. <https://doi.org/10.1175/JCLI-D-16-0257.1>
- Bodas-Salcedo, A., Webb, M. J., Bony, S., Chepfer, H., Dufresne, J.-L., Klein, S. A., et al. (2011). COSP: Satellite simulation software for model assessment. *Bulletin of the American Meteorological Society*, 92(8), 1023–1043. <https://doi.org/10.1175/2011BAMS2856.1>
- Boisvert, L. N., & Stroeve, J. C. (2015). The Arctic is becoming warmer and wetter as revealed by the Atmospheric Infrared Sounder. *Geophysical Research Letters*, 42, 4439–4446. <https://doi.org/10.1002/2015GL063775>
- Boucher, O., Randall, D. D., Artaxo, P., Bretherton, C., Feingold, G., Forster, P., et al. (2013). Chapter 7: Clouds and aerosols. In T. F. Stocker, et al. (Eds.), *Climate Change 2013: The Physical Science Basis. Contribution of Working Group I to the Fifth Assessment Report of the Intergovernmental Panel on Climate Change* (pp. 571–656). Cambridge, United Kingdom and New York, NY: Cambridge University Press.
- Ceppi, P., Hartmann, D. L., & Webb, M. (2016). Mechanisms of the negative shortwave cloud feedback in high latitudes. *Journal of Climate*, 29(1), 139–157. <https://doi.org/10.1175/JCLI-D-15-0327.1>
- Ceppi, P., Zelinka, M. D., & Hartmann, D. L. (2014). The response of the southern hemispheric eddy-driven jet to future changes in shortwave radiation in CMIP5. *Geophysical Research Letters*, 41, 3244–3250. <https://doi.org/10.1002/2014GL060043>
- Cesana, G., & Chepfer, H. (2013). Evaluation of the cloud thermodynamic phase in a climate model using CALIPSO-GOCCP. *Journal of Geophysical Research: Atmospheres*, 118, 7922–7937. <https://doi.org/10.1002/jgrd.50376>
- Chepfer, H., Bony, S., Winker, D., Cesana, G., Dufresne, J.-L., Minnis, P., et al. (2010). The GCM-Oriented CALIPSO Cloud Product (CALIPSO-GOCCP). *Journal of Geophysical Research*, 115, D00H16. <https://doi.org/10.1029/2009JD012251>
- Chepfer, H., Bony, S., Winker, D., Chiriaco, M., Dufresne, J.-L., & Sèze, G. (2008). Use of CALIPSO lidar observations to evaluate the cloudiness simulated by a climate model. *Geophysical Research Letters*, 35, L15704. <https://doi.org/10.1029/2008GL034207>
- Chepfer, H., Cesana, G., Winker, D., Getzewich, B., & Vaughan, M. (2013). Comparison of two different cloud climatologies derived from CALIOP level 1 observations: The CALIPSO-ST and the CALIPSO-GOCCP. *Journal of Atmospheric and Oceanic Technology*, 30(4), 725–744. <https://doi.org/10.1175/JTECH-D-12-00057.1>
- Choi, Y.-S., Kim, B.-M., Hur, S.-K., Kim, S.-J., Kim, J.-H., & Ho, C.-H. (2014). Connecting early summer cloud-controlled sunlight and late summer sea ice in the Arctic. *Journal of Geophysical Research: Atmospheres*, 119, 11,087–11,099. <https://doi.org/10.1002/2014JD022013>
- Curry, J. A., & Ebert, E. E. (1992). Annual cycle of radiation fluxes over the Arctic Ocean: Sensitivity to cloud optical properties. *Journal of Climate*, 5(11), 1267–1280. [https://doi.org/10.1175/1520-0442\(1992\)005<1267:ACORFO>2.0.CO;2](https://doi.org/10.1175/1520-0442(1992)005<1267:ACORFO>2.0.CO;2)
- Curry, J. A., Schramm, J. L., & Ebert, E. E. (1995). The sea ice-albedo climate feedback mechanism. *Journal of Climate*, 8(2), 240–247. [https://doi.org/10.1175/1520-0442\(1995\)008<0240:SIACFM>2.0.CO;2](https://doi.org/10.1175/1520-0442(1995)008<0240:SIACFM>2.0.CO;2)
- Dee, D. P., Uppala, S. M., Simmons, A. J., Berrisford, P., Poli, P., Kobayashi, S., et al. (2011). The ERA-Interim reanalysis: Configuration and performance of the data assimilation system. *The Quarterly Journal of the Royal Meteorological Society*, 137(656), 553–597. <https://doi.org/10.1002/qj.828>
- Deser, C., Tomas, R., Alexander, M., & Lawrence, D. (2010). The seasonal atmospheric response to projected Arctic Sea ice loss in the late twenty-first century. *Journal of Climate*, 23(2), 333–351. <https://doi.org/10.1175/2009JCLI3053.1>
- Frey, W. R., Maroon, E. M., Pendergrass, A., & Kay, J. E. (2017). Do Southern Ocean cloud feedbacks matter for 21st century warming? *Geophysical Research Letters*, 44, 12,447–12,456. <https://doi.org/10.1002/2017GL076339>
- Goosse, H., Kay, J. E., Armour, K. C., Bodas-Salcedo, A., Chepfer, H., Docquier, D., et al. (2018). Quantifying climate feedbacks in polar regions. *Nature Communications*, 9(1), 1919. <https://doi.org/10.1038/s41467-018-04173-0>
- Gordon, N., & Klein, S. A. (2014). Low-cloud optical depth feedback in climate models. *Journal of Geophysical Research: Atmospheres*, 119, 6052–6065. <https://doi.org/10.1002/2013JD021052>
- Guzman, R., Chepfer, H., Noel, V., Vaillant de Guelis, T., Kay, J. E., Raberanto, P., et al. (2017). Direct atmosphere opacity observations from CALIPSO provide new constraints on cloud-radiation interactions. *Journal of Geophysical Research: Atmospheres*, 122, 1066–1085. <https://doi.org/10.1002/2016JD025946>
- Hurrell, J. W., Holland, M. M., & Gent, P. R. (2013). The community Earth system model: A framework for collaborative research. *Bulletin of the American Meteorological Society*, 94(9), 1339–1360. <https://doi.org/10.1175/BAMS-D-12-00121.1>
- Jahn, A. (2018). Reduced probability of ice-free summers for 1.5°C compared to 2°C warming. *Nature Climate Change*, 8(5), 409–413. <https://doi.org/10.1038/s41558-018-0127-8>
- Kay, J. E., Bourdages, L., Miller, N. B., Morrison, A., Yettella, V., Chepfer, H., & Eaton, B. (2016). Evaluating and improving cloud phase in the community atmosphere model version 5 using spaceborne lidar observations. *Journal of Geophysical Research: Atmospheres*, 121, 4162–4176. <https://doi.org/10.1002/2015JD024699>
- Kay, J. E., Deser, C., Phillips, A., Mai, A., Hannay, C., Arblaster, J. M., et al. (2015). The community Earth system model (CESM) large ensemble project: A community resource for studying climate change in the presence of internal climate variability. *Bulletin of the American Meteorological Society*, 96(8), 1333–1349. <https://doi.org/10.1175/BAMS-D-13-00255.1>
- Kay, J. E., & Gettelman, A. (2009). Cloud influence on and response to seasonal Arctic Sea ice loss. *Journal of Geophysical Research*, 114, D18204. <https://doi.org/10.1029/2009JD011773>
- Kay, J. E., Hillman, B. R., Klein, S. A., Zhang, Y., Medeiros, B., Pincus, R., et al. (2012). Exposing global cloud biases in the community atmosphere model (CAM) using satellite observations and their corresponding instrument simulators. *Journal of Climate*, 25(15), 5190–5207. <https://doi.org/10.1175/JCLI-D-11-00469.1>
- Kay, J. E., Holland, M. M., Bitz, C. M., Blanchard-Wrigglesworth, E., Gettelman, A., Conley, A., & Bailey, D. (2012). The influence of local feedbacks and northward heat transport on the equilibrium Arctic climate response to increased greenhouse gas forcing. *Journal of Climate*, 25(16), 5433–5450. <https://doi.org/10.1175/JCLI-D-11-00622.1>
- Kay, J. E., L'Ecuyer, T., Chepfer, H., Loeb, N., Morrison, A., & Cesana, G. (2016). Recent advances in Arctic cloud and climate research. *Current Climate Change Reports*, 2(4), 159–169. <https://doi.org/10.1007/s40641-016-0051-9>
- Kay, J. E., Raeder, K., Gettelman, A., & Anderson, J. (2011). The boundary layer response to recent Arctic sea ice loss and implications for high-latitude climate feedbacks. *Journal of Climate*, 24(2), 428–447. <https://doi.org/10.1175/2010JCLI3651.1>

- Klein, S. A., & Hartmann, D. L. (1993). The seasonal cycle of low stratiform clouds. *Journal of Climate*, 6(8), 1587–1606. [https://doi.org/10.1175/1520-0442\(1993\)006<1587:TSCOLS>2.0.CO;2](https://doi.org/10.1175/1520-0442(1993)006<1587:TSCOLS>2.0.CO;2)
- Klein, S. A., Zhang, Y., Zelinka, M., Pincus, R., Boyle, J., & Glecker, P. J. (2013). Are climate model simulations of clouds improving? An evaluation using the ISCCP simulator. *Journal of Geophysical Research: Atmospheres*, 118, 1329–1342. <https://doi.org/10.1002/jgrd.50141>
- Koenigk, T., Brodeau, L., Graverson, R. G., Karlsson, J., Svensson, G., Tjernstrom, M., et al. (2013). Arctic climate change in 21st century CMIP5 simulations with EC-Earth. *Climate Dynamics*, 40(11–12), 2719–2743. <https://doi.org/10.1007/s00382-012-1505-y>
- Lawrence, D. M., Slater, A. G., Tomas, R. A., Holland, M. M., & Deser, C. (2008). Accelerated Arctic land warming and permafrost degradation during rapid sea ice loss. *Geophysical Research Letters*, 35, L11506. <https://doi.org/10.1029/2008GL033985>
- Manabe, S., & Stouffer, R. (1980). Sensitivity of a global climate model to an increase of CO₂ concentration in the atmosphere. *Journal of Geophysical Research*, 85(C10), 5529–5554. <https://doi.org/10.1029/JC085iC10p05529>
- McDougall, T. J., & Barker, P. M. (2011). Getting started with TEOS-10 and the Gibbs seawater (GSW) oceanographic toolbox, 28pp., SCOR/IAPSO WG127, ISBN 978-0-646-55621-5
- McLhattan, E., L'Ecuyer, T., & Miller, N. B. (2017). Observational evidence linking Arctic supercooled liquid cloud biases in CESM to snowfall processes. *Journal of Climate*, 30(12), 4477–4495. <https://doi.org/10.1175/JCLI-D-16-0666.1>
- Morrison, A. L., Kay, J. E., Chepfer, H., Guzman, R., & Yettella, V. (2018). Isolating the liquid cloud response to recent Arctic Sea ice variability using spaceborne lidar observations. *Journal of Geophysical Research: Atmospheres*, 123, 473–490. <https://doi.org/10.1002/2017JD027248>
- Morrison, H., de Boer, G., Feingold, G., Harrington, J., Shupe, M. D., & Sulia, K. (2012). Resilience of persistent Arctic mixed-phase clouds. *Nature Geoscience*, 5(1), 11–17. <https://doi.org/10.1038/ngeo1332>
- Neale, R. B., Chen, C.-C., Gettelman, A., Lauritzen, P. H., Park, S., Williamson, D. L., et al. (2012). Description of the NCAR Community Atmosphere Model (CAM5). Technical Report NCAR/TN-486+STR. National Center for Atmospheric Research, Boulder, Colorado, 268 pp.
- Pendergrass, A., Conley, A., & Vitt, F. (2018). Surface and top-of-atmosphere radiative feedback kernels for CESM-CAM5. *Earth System Science Data*, 10(1), 317–324. <https://doi.org/10.5194/essd-10-317-2018>
- Pithan, F., & Mauritsen, T. (2014). Arctic amplification dominated by temperature feedbacks in contemporary climate models. *Nature Geoscience*, 7(3), 181–184. <https://doi.org/10.1038/ngeo2071>
- Serreze, M. C., & Barry, R. (2011). Processes and impacts of Arctic amplification: A research synthesis. *Global and Planetary Change*, 77(1–2), 85–96. <https://doi.org/10.1016/j.gloplacha.2011.03.004>
- Shell, K. M., Kiehl, J. T., & Shields, C. A. (2008). Using the radiative kernel technique to calculate climate feedbacks in NCAR's community atmospheric model. *Journal of Climate*, 21(10), 2269–2282. <https://doi.org/10.1175/2007JCLI2044.1>
- Shupe, M. D., & Intrieri, J. (2004). Cloud radiative forcing of the Arctic surface: The influence of cloud properties, surface albedo, and solar zenith angle. *Journal of Climate*, 17(3), 616–628. [https://doi.org/10.1175/1520-0442\(2004\)017<0616:CRFOTA>2.0.CO;2](https://doi.org/10.1175/1520-0442(2004)017<0616:CRFOTA>2.0.CO;2)
- Smith, R. D., Jones, P., Briegleb, B., Bryan, F., Danabasoglu, G., Dennis, J., Dukowicz, J., et al. (2010). The Parallel Ocean Program (POP) reference manual: Ocean component of the Community Climate System Model (CCSM) and Community Earth System Model (CESM). Los Alamos National Laboratory Technical Report LAUR-10-01853, 141 pp. Retrieved from www.cesm.ucar.edu/models/cesm1.0/pop2/doc/sci/POPRefManual.pdf
- Soden, B., Held, I. M., Colman, R., Shell, K. M., Kiehl, J. T., & Shields, C. A. (2008). Quantifying climate feedbacks using radiative kernels. *Journal of Climate*, 21(14), 3504–3520. <https://doi.org/10.1175/2007JCLI2110.1>
- Soden, B., & Vecchi, G. (2011). The vertical distribution of cloud feedback in coupled ocean-atmosphere models. *Geophysical Research Letters*, 38, L12704. <https://doi.org/10.1029/2011GL047632>
- Sorteberg, A., Kattsov, V., Walsh, J. E., & Pavlova, T. (2007). The Arctic surface energy budget as simulated with the IPCC AR4 AOGCMs. *Climate Dynamics*, 29(2–3), 131–156. <https://doi.org/10.1007/s00382-006-0222-9>
- Stroeve, J. C., Kattsov, V., Barrett, A., Serreze, M., Pavlova, T., Holland, M., & Meier, W. N. (2012). Trends in Arctic sea ice extent from CMIP5, CMIP3 and observations. *Geophysical Research Letters*, 39, L16502. <https://doi.org/10.1029/2012GL052676>
- Taylor, K. E., Crucifix, M., Braconnot, P., Hewitt, C. D., Doutriaux, C., Broccoli, A. J., Mitchell, J. F. B., et al. (2007). Estimating shortwave radiative forcing and response in climate models. *Journal of Climate*, 20(11), 2530–2543. <https://doi.org/10.1175/JCLI4143.1>
- Taylor, K. E., Stouffer, R. J., & Meehl, G. A. (2012). The CMIP5 experiment design. *Bulletin of the American Meteorological Society*, 93(4), 485–498. <https://doi.org/10.1175/BAMS-D-11-00094.1>
- Taylor, P. C., Hegyi, B. M., Boeke, R. C., & Boisvert, L. N. (2018). On the increasing importance of air-sea exchanges in a thawing Arctic: A review. *Atmosphere*, 9(2). <https://doi.org/10.3390/atmos9020041>
- Vaillant de Guelis, T., Chepfer, H., Noel, V., Guzman, R., Winker, D. M., & Plougonven, R. (2017). Using space lidar observations to decompose longwave cloud radiative effect variations over the last decade. *Geophysical Research Letters*, 44, 11,994–12,003. <https://doi.org/10.1002/2017GL074628>
- Vavrus, S., Bhatt, U., & Alexeev, V. (2011). Factors influencing simulated changes in future Arctic cloudiness. *Journal of Climate*, 24(18), 4817–4830. <https://doi.org/10.1175/2011JCLI4029.1>
- Vavrus, S., Waliser, D., Schweiger, A., & Francis, J. A. (2009). Simulations of 20th and 21st century Arctic cloud amount in the global climate models assessed in the IPCC AR4. *Climate Dynamics*, 33(7–8), 1099–1115. <https://doi.org/10.1007/s00382-008-0475-6>
- Webb, M. J., Andrews, T., Bodas-Salcedo, A., Bony, S., Bretherton, C. S., Chadwick, R., et al. (2017). The Cloud Feedback Model Intercomparison Project (CFMIP) contribution to CMIP6. *Geoscience Model Development*, 10(1), 359–384. <https://doi.org/10.5194/gmd-10-359-2017>
- Wesslén, C., Tjernström, M., Bromwich, D. H., de Boer, G., Ekman, A. M. L., Bai, L.-S., & Wang, S. H. (2014). The Arctic summer atmosphere: An evaluation of reanalyses using ASCOS data. *Atmospheric Chemistry and Physics*, 14(5), 2605–2624. <https://doi.org/10.5194/acp-14-2605-2014>
- Winton, M. (2006). Amplified Arctic climate change: What does surface albedo feedback have to do with it? *Geophysical Research Letters*, 33, L03701. <https://doi.org/10.1029/2005GL025244>
- Zelinka, M., Klein, S. A., & Hartmann, D. L. (2012). Computing and partitioning cloud feedbacks using cloud property histograms. Part II: Attribution to changes in cloud amount, altitude, and optical depth. *Journal of Climate*, 25(11), 3736–3754. <https://doi.org/10.1175/JCLI-D-11-00249.1>